Appl. Phys. B (2013) 110:425–431
DOI 10.1007/s00340-012-5272-6

Applied Physics B
Lasers and Optics

Optical parametric oscillator pumped by relaxation oscillation pulses of a mechanically Q-switched Nd:YAG laser

Saeed Ghavami Sabouri · Alireza Khorsandi

Received: 24 July 2012 / Revised: 8 November 2012 / Published online: 24 November 2012

Abstract We report the generation of mid-infrared pulsed radiation between 2.2 and 3 μm range using a singly-resonant optical parametric oscillator (SR-OPO) based on a 40-mm-long crystal of periodically-poled $LiNbO_3$ (PPLN) pumped by mechanically Q-switched pulses from a Nd:YAG laser, obtained by chopping the beam inside the laser resonator over a 1–10 kHz duty cycle. An appreciable reduction in pulse width as well as the number of relaxation oscillation pulses of the Nd:YAG pump laser is observed when the frequency of the Q-switch chopper is increased up to 10 kHz. Sub-nanosecond relaxation oscillation pulses of about 170–210 ns duration are generated under the width of the idler envelope varying from 4.6 to 8.55 μs. The same behavior is observed for the signal wave. A maximum extraction efficiency of 22 % is obtained for the idler, corresponding to 785 mW of output power at 10 kHz. The tuning of the signal and idler beams were performed by temperature variation of the PPLN crystal within 100–200 °C range.

1 Introduction

The unique characteristics of optical parametric oscillators (OPO) including wide tuning range and large optical bandwidth makes them very attractive, efficient, and powerful coherent light source for many applications in different spectral regions from the visible to mid-infrared (mid-IR) [1]. Compared with the doubly-resonant OPO (DR-OPO) scheme, the singly-resonant OPO (SR-OPO) configuration is potentially capable of providing low frequency jitter and drift, improved passive stability, as well as high conversion efficiencies exceeding 90 %, if supported by an adequate pumping level above threshold [2]. Recently, new fiber laser sources with relatively good beam quality and high output power have been introduced for pumping SR-OPOs in the cw regime, with total output powers of as much as 17.5 W generated in the near- and mid-IR region [3]. At the same time, owing to the high spectral purity, sufficient output power, widespread availability, and the capability of operating in different temporal regimes, from cw to the picosecond time-scale, diode-pumped Nd:YAG lasers still remain very efficient, compact, and high-performance pump sources for a variety of mid-IR OPO devices based on quasi-phase-matched (QPM) nonlinear crystals such as periodically-poled $LiNbO_3$ (PPLN) [4].

Such radiation is suitable for spectroscopic applications in environmental [5] and medical diagnostic [6], as well as high-power mid-IR LIDARs [7]. However, for many applications including material breakdown phenomena and long-distance LIDAR measurement of wind velocity [8] much more energetic OPO pulses having longer duration than 10–100 ns produced by conventional Q-switched Nd:YAG pumped OPOs are required. While the Nd:YAG pump can operate in high-power mode, relaxation oscillation spikes with variable pulse widths on the order of nanoseconds can be presented at the beginning of the laser operation. Depending on the excitation process and Q-switching scheme, pulse width and repetition rate of these spikes can be accurately controlled. Recently, gain-switched picosecond laser diode with a relatively wide range of pulse widths from 20 ps to 2 ns [9], and high-power gain-switched Tm^{3+}-doped fiber laser with 75 ns–1 μs of

S. Ghavami Sabouri (✉) · A. Khorsandi
Department of Physics, University of Isfahan,
81746-73441 Isfahan, I.R. Iran
e-mail: ghavami@sci.ui.ac.ir

pulse width and variable repetition rate of 500 Hz–50 kHz have been reported [10].

On the other hand, in a typical slow Q-switching scheme based on, for example, mechanical modulation of the laser beam, it is possible to generate a relatively long microsecond envelope containing several relaxation oscillation spikes of nanosecond duration. In the present paper, to the best of our knowledge, we report for the first time a SR-OPO pumped by the relaxation oscillation pulses of a high-power, slowly Q-switched Nd:YAG laser. A mechanical chopper with a variable duty cycle over 1–10 kHz is used inside the cavity of a high-power cw Nd:YAG laser to produce a train of nanosecond relaxation pulses inside a microsecond Q-switched envelope of the laser output. The generated pulses are then used to pump a SR-OPO ring cavity containing a 40 mm crystal of PPLN as the nonlinear gain medium to obtain a mid-IR idler wave between 2.2 and 3 μm with variable pulse length of about 170–210 ns and the repetition rate of 10–1 kHz. A maximum idler conversion efficiency of 22 % is measured corresponding to an idler output power of 785 mW.

2 Experimental setup

A schematic of the experimental setup of the SR-OPO pumped by the relaxation oscillation (RO) pulses of the mechanically Q-switched high-power Nd:YAG laser is depicted in Fig. 1.

The Nd:YAG laser utilized a 64-mm-long cylindrical crystal rod with a diameter of 4 mm as the active medium. Laser pumping was provided by three bars of diode arrays located on the top of a triangular around the Nd:YAG rod to permit side-pumping of the crystal. By varying the injection current up to 18 A and hence modulating the output power of the diodes, a maximum Nd:YAG output power of 6 W was achieved when the laser was operated in the cw mode. The entire laser system was packed in a quartz jacket, and double-ionized pure water with the capacity of about 6 lit/min was circulated inside the jacket to minimize thermal fluctuations in the Nd:YAG laser output intensity. Two plane mirrors were coated to provide reflectivity of 99.95 and 80 % at 1064.2 nm, as the input and output cavity mirrors, respectively. An optimum cavity length of about 40 cm was then provided to achieve the highest beam quality in the Nd:YAG laser output beam. The measurement of the M^2 quality factor of the laser beam was performed according to the ISO standard [11]. This resulted in values of $M_x^2 = 1.4$ and $M_y^2 = 1.5$, confirming a nearly TEM00 Gaussian profile, thus allowing optimum mode-matching to the resonant signal beam for maximum parametric gain in the PPLN crystal. A dielectric coated thin slab of glass was used as polarizer inside the cavity and oriented at Brewster angle to establish the required

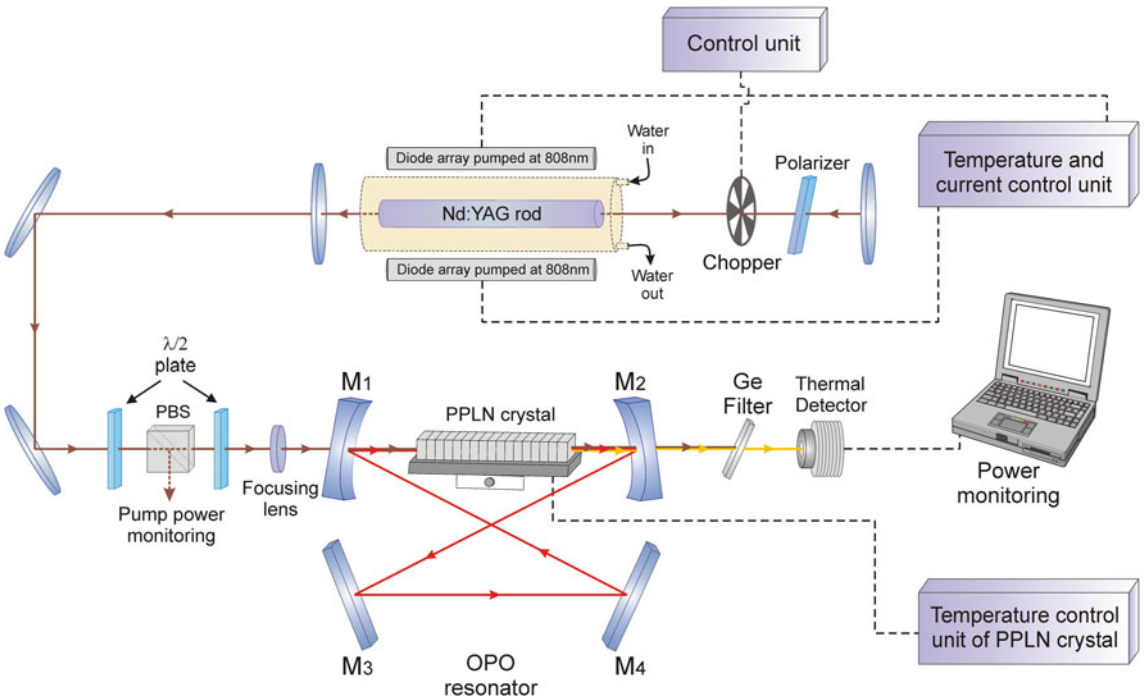

Fig. 1 Schematic of the experimental setup of the SR-OPO pumped by relaxation oscillation pulses generated by the slowly mechanically Q-switched high-power Nd:YAG laser

extraordinary Nd:YAG beam for parametric generation in the PPLN crystal.

Pulsing of the Nd:YAG laser was performed simply by mechanical chopping of the beam inside the cavity. The utilized chopper contained 45 identical slots to strike the laser beam at a nearly stable frequency of 1–10 kHz duty cycle. Accurate measurement of the duration of the generated RO output pulses was performed using a InGaAs fast photodiode with 100 ps rise time (Thorlabs, FGA04, sensitivity over 800–1800 nm). A thermal detector (Thorlabs PM100 & DCMM) was also used to measure the output power of the Q-switched Nd:YAG laser beam after passing through a polarizing beam-splitter (PBS).

The characterization of the Nd:YAG RO pulses is shown in Fig. 2. As can be seen, when the chopper frequency is increased to 10 kHz, the number of RO pulses decreases to one with almost all the power contained in the fundamental spike. Following theoretical analysis [12], it can be concluded that the RO pulses decay more rapidly in time as the number of the spikes decreases which is in excellent agreement with the obtained experimental results shown in Fig. 2. However, the oscillation decay time as well as the number of oscillating pulses are strongly dependent on the population inversion and the photon flux inside the cavity of the Nd:YAG laser [13]. These can be controlled by proper choice of the Q-switching rate, which in turn depends on the chopper frequency.

As the chopper frequency is increased from 1 to 10 kHz, a moderate decrease in the RO pulse duration from $\sim$210 to $\sim$170 ns is also observed. Similarly, a reduction from $\sim$8.55 μs at 1 kHz to $\sim$4.6 μs at 10 kHz is measured for the Q-switched output pulse envelope. While the mechanically Q-Switched Nd:YAG laser beam is deployed

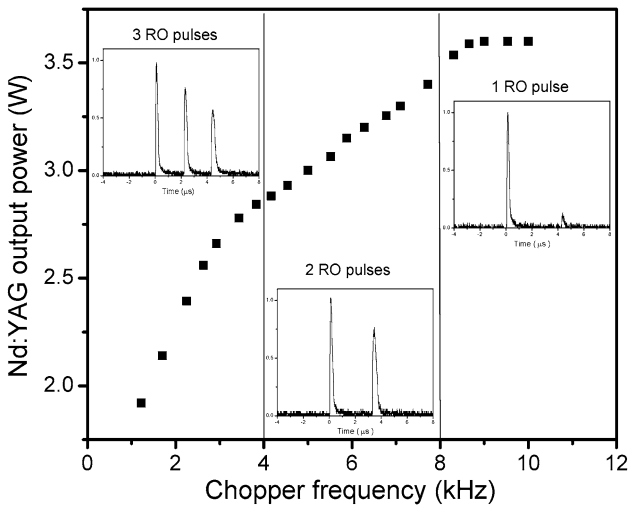

Fig. 2 Characteristics of the Nd:YAG RO pulses. The output power as well as the number of the Nd:YAG RO pulses change with the chopper frequency

to pump the SR-OPO, only the RO pulses that contain sufficient peak power well above the OPO threshold can contribute to the generation of parametric waves inside the PPLN nonlinear crystal. The maximum average output power of the Nd:YAG laser was 3.6 W at a chopper frequency of 1 kHz, increasing to a maximum value of 1.9 W at a 10 kHz.

The SR-OPO cavity consisted of two concave mirrors and two plane mirrors, all with CaF_2 substrates. The curvature of the concave mirrors, M_1 and M_2, was $r = -20$ cm. All cavity mirrors were anti-reflection (AR)-coated for pump and idler wavelengths over the range 2200–5000 nm and coated for high reflectivity over the signal wavelength range of 1450–2100 nm. To ensure the pump beam polarization was matched for $e \rightarrow e + e$ interaction in the PPLN crystal, a half-wave-plate in combination with a PBS cube were utilized before entry into the SR-OPO cavity. The Q-switched Nd:YAG laser pump beam was then focused into the PPLN crystal using an uncoated lens of focal length, $f = 20$ cm. This provided a minimum spot size of $w_0 \sim 50\,\mu$m at the center of the PPLN crystal, corresponding to a focusing parameter of $\xi \sim 1.2$. The PPLN crystal was 40-mm-long, 10-mm-wide and 0.5-mm-thick and contained nine uniform gratings of 500 μm width across the 10 mm aperture. The period of the gratings varied from 29.50 to 31.75 μm in 0.25 μm steps. The crystal faces were AR-coated ($R < 1$ %) at the pump, signal and idler wavelengths. We only utilized two gratings with periods of 31 and 30.75 μm in the experiment.

Excitation of the PPLN generates a low-power frequency-doubled green light at 532 nm that can be used to align the OPO mirrors. At the beginning of OPO action, the resonated signal is the sum-frequency (SF) mixed with the pump to generate about 5 mW of red light. The tunability of the SF beam generated from the 30.75 μm grating channel was from 651.6 to 673.3 nm, and that generated from the 31 μm channel was from 660.58 to 693.4 nm. The tuning of the SR-OPO was achieved by changing the temperature of the PPLN crystal within the 100–200 °C range. The temperature was accurately controlled to avoid photorefractive effect during operation. It was performed by a thermoelectric device (TC200, Thorlabs Co.) with an accuracy of $\Delta T = \pm 0.1$°C. Signal and idler wavelengths were estimated for both gratings using the non-phase-matched sum-frequency wavelengths generated in the visible, as the temperature was varied. The experimental results as well as theoretical tuning curves are shown in Fig. 3. As can be seen from the plot, the measured data are in good agreement with theoretical tuning curves calculated from the Sellmeier equations of the material [14].

The RO pulses generated from the Nd:YAG laser provided an average power of about 2.6 W at 3 kHz. This was found to readily exceed the threshold power of the

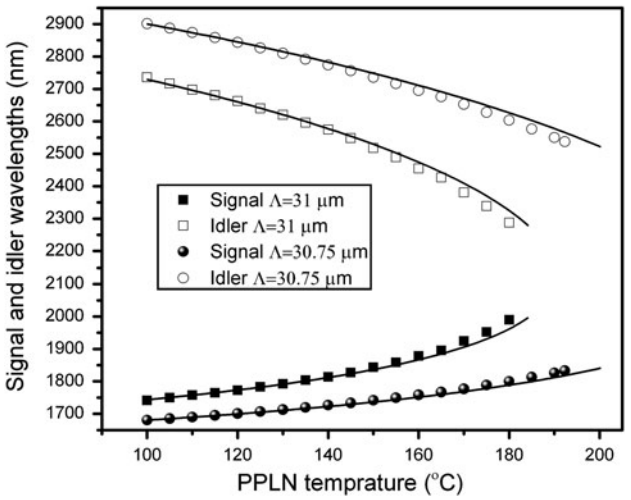

Fig. 3 Tuning characteristics of the signal and idler waves through changing of the PPLN temperature in 100–200 °C for both $\Lambda = 30.75$ μm and $\Lambda = 31$ μm channels of the crystal. Theoretical data are based on the Sellemier equations for the material [14]

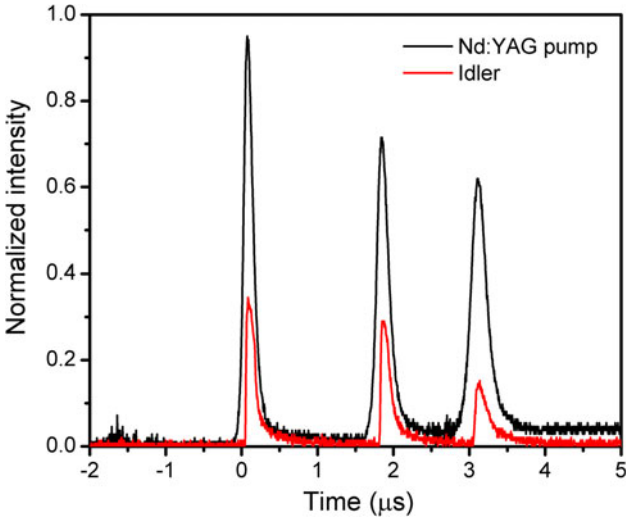

Fig. 4 Generated idler beam by three RO pulses emitted from the mechanical Q-switched Nd:YAG laser pump with the chopper frequency kept at 4 kHz. The pulse shapes are captured by InGaAs fast photodiode. The extreme PPLN grating channel with 31 μm period is used

SR-OPO measured to be 1.5 W at a chopper frequency of 1 kHz. Therefore, under this condition, even the low-power secondary RO pulses oscillating over 1–4 kHz of chopper frequency were able to generate signal and idler output pulses. Tuning characterization of the signal from 1680 to 1990 nm and the idler from 2287 to 2901 nm was performed by temperature tuning the PPLN crystal up to 200 °C for both grating periods utilized.

Figure 4 shows typical temporal profile of the generated idler pulses together with the depleted RO pulses at the output of the SR-OPO cavity. As evident from the figure, the generated idler pulses follow the oscillation of the RO pump pulses and decay in nearly the same manner, while most of the power is down-converted from the fundamental spike. Moreover, for the first RO pulse, the idler pulse has a faster rise time than the subsequent RO pulses, as expected, due to the higher peak power. In fact, the generated idler pulses exhibit good correlation with the three RO pump pulses both in duration and rise time. The rise time associated with the first RO spike is measured as ~ 17 ns for the idler and ~ 88 ns for the pump pulse. These values increase to ~ 20 and ~ 115 ns for the second RO pulses, and to ~ 24 and ~ 150 ns for the third spike. These confirm the significant pulse narrowing from the pump to SR-OPO output, resulting in nanosecond idler pulses.

We also characterized the spatial quality of the idler output pulses using the same technique as used for the Nd:YAG pump beam [10], resulting in a beam quality factor of $M^2 = 1.7$. In addition, we investigated the depletion of the pump power to determine the maximum down-conversion efficiency from the pump to the parametric waves. Figure 5 shows the measured pump depletion as a function of chopper frequency from 1 to 10 kHz. As clearly seen from the plot, the down-conversion efficiency rises with the increase in the chopper frequency, reaching a maximum value of 59 % at a frequency of 10 kHz. This can be correlated with the results deduced from Fig. 2, where at Q-switching frequencies higher than 8 kHz the only fundamental spike is the dominant oscillating pulse.

The effect of the modulation frequency on the duration of the pump and the generated idler pulses was also investigated, with the results shown in Fig. 6. As can be

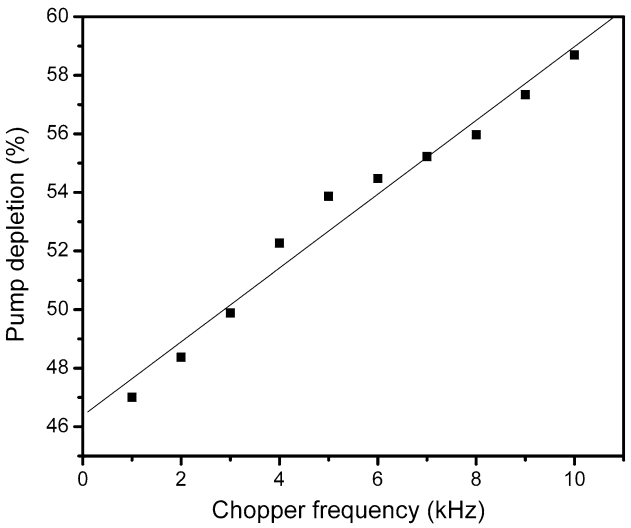

Fig. 5 Variation of the Nd:YAG pump depletion with increasing the Q-switching frequency. Pump depletion rises almost linearly as the Q-switch chopper frequency is increased from 1 to 10 kHz

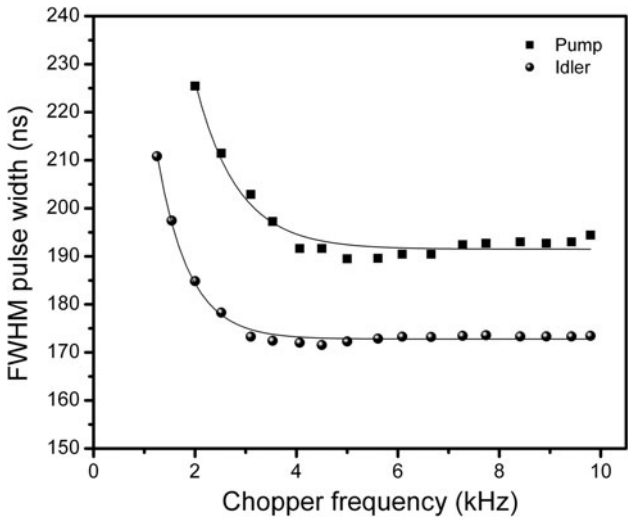

Fig. 6 Measured RO pump and SR-OPO idler pulse duration (FWHM) versus chopper frequency during Q-switching of the Nd:YAG laser with the PPLN grating period of 31 μm

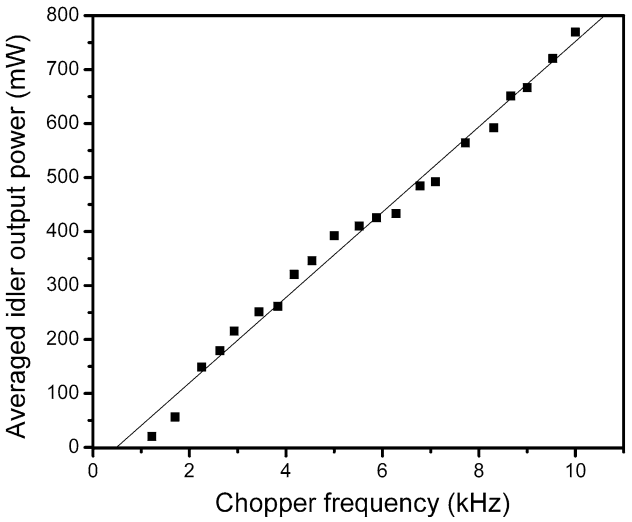

Fig. 8 Variation of the idler output power with the frequency of the Q-switching chopper for 31 μm grating period. The output power exhibits strong growth as the chopper frequency is increased to 10 kHz

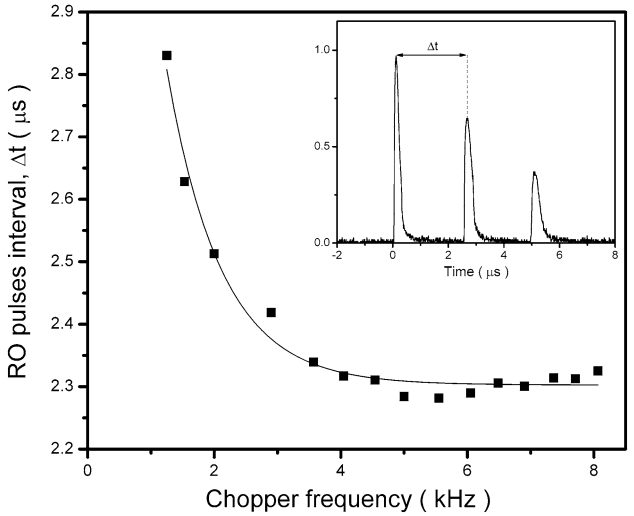

Fig. 7 Variation of time between of two consecutive SR-OPO idler pulses generated from 31 μm grating period. The measurements were performed for modulation frequencies below 8 kHz, where at least two RO pulses could oscillate

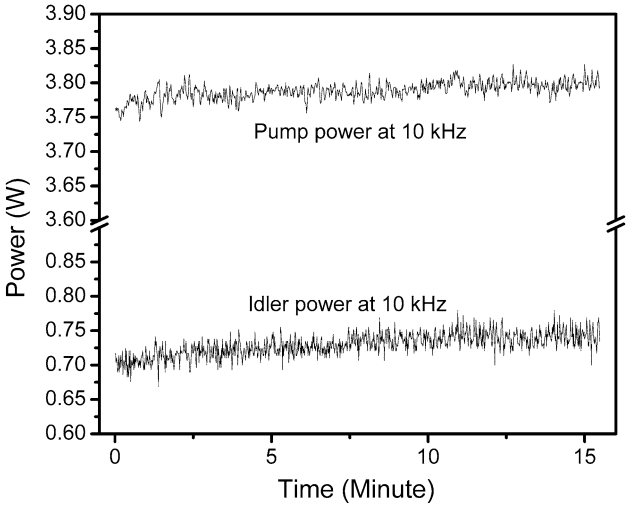

Fig. 9 Power fluctuations of the Nd:YAG pump and generated idler during 15 min of data acquisition, while operating at their maximum power at 10 kHz of chopper frequency

seen, while the Q-switching modulation frequency is increased to 3 kHz, the FWHM pump pulse width decreases from ~225 to ~190 ns. A significant reduction is similarly obtained for the idler pulses starting from ~210 ns down to ~170 ns. However, no significant change in the pulse width of the pump and idler envelope were observed. Beyond 3 kHz, the pump and idler pulses exhibit relatively steady-state values of ~189 and ~179 ns, respectively. For frequencies below 3 kHz, broader idler pulses in the 170–210 ns range are obtained.

The feasibility of varying the repetition rate and pulse width of the generated SR-OPO output as a function of the chopper frequency is illustrated in Fig. 7. As can be seen, the time interval between sequence RO pulses can vary from $\Delta t \sim$ 2.3 μs to about $\Delta t \sim$ 2.8 μs. The time interval, Δt, strongly depend on the photon flux circulating in the resonator, which in turn determines the number of RO pulses under the Q-switched envelope.

A novel advantage of the SR-OPO described here is that for a fixed idler pulse width, the average idler output power can be enhanced by increasing the chopper frequency. This attractive behavior is depicted in Fig. 8. The data were obtained after taking into account all possible losses due to the coatings and the germanium filter. The increase in average idler power at higher frequencies is mainly due to

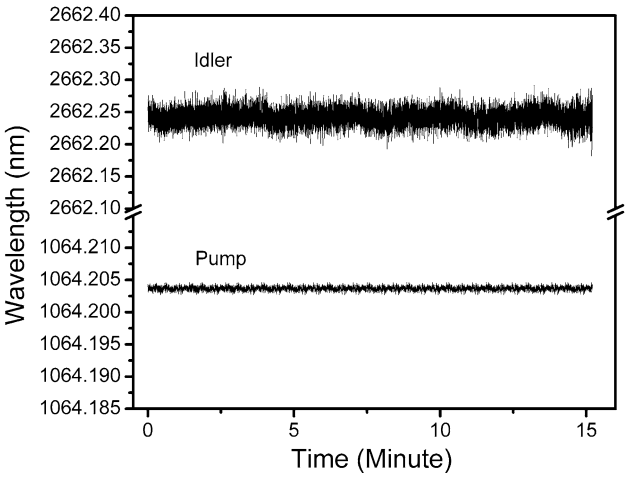

Fig. 10 Pump and idler frequency fluctuations during 15 min data acquisition. Idler wavelengths is estimated using the red sum-frequency wavelength measurement through the utilized accurate wave meter

the suppression of additional RO pulses other than the fundamental spike. It can be further verified from the plot that beyond 3 kHz of chopper frequency, where the RO pump pulse width is nearly constant, the idler output power increases up to 785 mW, again due to the increasing suppression of additional RO pulses beyond the fundamental spike.

Compared with the alternative mid-IR laser sources, the generated SR-OPO output can be advantageous in improving depth resolution of many spectroscopic targets as well as sensitive medical diagnostics [6]. On the other hand, in addition to the spectral purity and adequate tuning characteristics high-resolution spectroscopy requires laser sources possessing long-term power stability and minimum frequency fluctuations. However, the power and spectral stability of the generated idler pulses is strongly dependent on the stability of the RO pump pulses. In Fig. 9, the results of stability measurements on the average idler power is shown. As can be seen, the fluctuations in the pump and idler rms output power are measured to be below 2 %.

We also performed measurements of spectral stability for both the idler and pump, with the results illustrated in Fig. 10. The measurements were performed using a wavemeter (Bristol 821) possessing absolute accuracy of ±0.6 GHz and a repeatability of ±0.06 GHz, as provided by the manufacturer. As can be seen from the plot, the idler frequency exhibits very good stability with an average fluctuation of about ±0.05 nm over 15 min, while the pump frequency remains stable within ±120 MHz.

3 Conclusion

We have thus demonstrated, for the first time to our knowledge, the generation of mid-IR idler pulses from a SR-OPO based on PPLN pumped by a mechanically Q-switched Nd:YAG laser providing relaxation oscillation pulses of 230–190 ns at 1–10 kHz repetition rate. The generated idler pulses exhibit durations of 210–170 ns over 1–10 kHz repetition rate and provide a maximum average power of 785 mW in 170 ns pulses at 10 kHz, corresponding to a maximum idler extraction efficiency of 22 % for 3.6 W of average pump power. An idler tuning range over 2287–2901 nm and a corresponding signal range of 1680–1990 nm are achieved by temperature tuning the PPLN crystal. The effect of the Q-switching frequency on the pulse width and number of the relaxation spikes has also been considered and characterized. It has been found that due to the narrowing of pulse envelope the number of relaxation oscillation pulses reduces to one as the chopper frequency is increased to 10 kHz, resulting in minimum SR-OPO oscillation threshold and maximum idler output power. The SR-OPO also exhibits very good output power and spectral stability, making it a viable and practical source for a variety of spectroscopic and medical applications.

References

1. T. Debuisschert, Nanosecond optical parametric oscillators. Quantum Semiclassical Opt.: J. Eur. Opt. Soc. Part B **9**(2), 209 (1997)
2. M. Ebrahim-Zadeh, in *Mid-Infrared Optical Parametric Oscillators and Applications Mid-Infrared Coherent Sources and Applications*, eds. by M. Ebrahim-Zadeh and I.T. Sorokina. (Springer, Netherlands, 2008), pp. 347–375
3. S. Chaitanya Kumar et al., Optimally-output-coupled, 17.5 W, fiber-laser-pumped continuous-wave optical parametric oscillator. Appl. Phys. B: Lasers O. **102**(1), 31–35 (2011)
4. Z. Jiao et al., High average power 2 μm generation using an intracavity PPMgLN optical parametric oscillator. Opt. Lett. **37**(1), 64–66 (2012)
5. Y. He et al., Spectroscopic applications of optical parametric oscillators. Opt. Photon. News **13**(5), 56–60 (2002)
6. D.D. Arslanov et al., Real-time, subsecond, multicomponent breath analysis by optical parametric oscillator based off-axis integrated cavity output spectroscopy. Opt. Express **19**(24), 24078–24089 (2011)
7. M. Raybaut et al., High-energy single-longitudinal mode nearly diffraction-limited optical parametric source with 3 MHz frequency stability for CO2 DIAL. Opt. Lett. **34**(13), 2069–2071 (2009)
8. J. Harrison, G.A. Rines, P.F. Moulton, Long-pulse generation with a stable-relaxation-oscillation Nd:YLF laser. Opt. Lett. **13**(4), 309–311 (1988)
9. A. Fragemann, V. Pasiskevicius, F. Laurell, Optical parametric amplification of a gain-switched picosecond laser diode. Opt. Express **13**(17), 6482–6489 (2005)
10. Y. Tang et al., High-power gain-switched Tm3+-doped fiber laser. Opt. Express **18**(22), 22964–22972 (2010)
11. D. Wright et al., Laser beam width, divergence and beam propagation factor—an international standardization approach. Opt. Quant. Electron. **24**(9), S993–S1000 (1992)

12. W. Koechner, *Solid-State Laser Engineering*, 6th edn., Springer Series in Optical Sciences (Springer, New York, 2006), p. 748
13. H. Statz et al., Problem of spike elimination in lasers. J. Appl. Phys. **36**(5), 1510–1514 (1965)
14. D.H. Jundt, Temperature-dependent Sellmeier equation for the index of refraction, ne, in congruent lithium niobate. Opt. Lett. **22**(20), 1553–1555 (1997)